BMC Cancer

RESEARCH Open Access

Correlation between METTL3 overexpression and ^{18}F-FDG uptake in patients with soft tissue sarcoma

Tong Wu[1], Jinghui Xie[1], Hongbo Feng[1], Hua Zhang[1], Juan Tao[2] and Bo Chen[1*]

Abstract

Background N6-methyladenosine (m6A) methylation plays a key role in tumor progression. However, the significance of methyltransferase-like 3 (METTL3) in biological processes of soft tissue sarcoma (STS) patients, and the relationship between METTL3 and STS are unclear.

Methods The expression of METTL3 in STS and its relationship with patient prognosis were determined from database analyses. Immunohistochemical staining and ^{18}F-FDG radioautography were performed on tumor tissues from 39 patients with STS undergoing ^{18}F-FDG PET before treatment. METTL3 expression in tumor and peritumoral tissues was evaluated with the Wilcoxon test. The Mann-Whitney *U* test and Spearman's correlation analysis were used to explore correlations of METTL3 expression with both clinicopathological characteristics and ^{18}F-FDG uptake. One-way analysis of variance and ROC analysis were used to evaluate the efficacy of ^{18}F-FDG PET metabolic parameters in predicting METTL3 expression.

Results METTL3 expression was significantly higher in STS tumor tissues than normal tissues (all p values<0.01), and correlated with poor patient prognosis ($p < 0.05$). METTL3 expression was associated with histological differentiation (Z=-2.026, $p = 0.043$), but no significant difference was observed according to age, sex, tumor size, tumor location, or metastasis (all p values > 0.05). METTL3 expression positively correlated with the expression of CD163 ($r = 0.502$, $p = 0.011$), CD68 ($r = 0.381$, $p = 0.017$), and CD8 ($r = 0.319$, $p = 0.048$), and exhibited a trend toward correlation with CD4 expression ($r = 0.310$, $p = 0.055$). Moreover, ^{18}F-FDG metabolism positively correlated with METTL3 expression in STS ($r = 0.580$ for PET and $r = 0.434$ for radioautography, all p values<0.01). The SUVmax of PET was significantly higher in tumors with high rather than low METTL3 expression (Z=-2.979, $p = 0.003$).

Conclusions METTL3 was overexpressed in STS, which may be a meaningful target of action in STS patients. The ^{18}F-FDG uptake was significantly elevated in tumors with high METTL3 expression, SUVmax could provide a meaningful imaging biomarker for its expression.

Keywords Soft tissue sarcomas, Methyltransferase-like protein 3, ^{18}F-fluorodeoxyglucose, Immune cell infiltration

*Correspondence:
Bo Chen
chenbojobs@163.com
[1]First Affiliated Hospital of Dalian Medical University, Dalian, China
[2]Second Affiliated Hospital of Dalian Medical University, Dalian, China

Introduction

Soft tissue sarcoma (STS) are rare, heterogeneous mesenchymal malignancies [1]. In recent years, substantial progress has been made in the multidisciplinary diagnosis and treatment of STS [2]. However, approximately 25% of patients with STS experience distant metastasis, and the metastasis rate has increased to approximately 50% of high grade STS [3]. Thus, increasing the effectiveness of patient treatment strategies and improving clinical outcomes have been major challenges requiring exploration of novel strategies against STS.

The N6-methyladenosine (m6A) is among the most prevalent RNA modifications regulating RNA metabolism [4]. The roles of methyltransferase-like 3 (METTL3), a core catalytic subunit of m6A regulators, have been widely studied in other tumors. METTL3 is overexpressed in various human malignant tumors and plays a role in regulating cancer progression through multiple mechanisms [5, 6]. However, the relationship between m6A modifications and STS remains unclear.

The "Warburg effect" is a crucial aspect of metabolic reprogramming in human malignant tumors. Several studies have highlighted links between specific epigenetic factors and glucose metabolism [7, 8]. Our previous research has demonstrated a strong correlation between ^{18}F-FDG metabolism in patients with STS and the level of immune cell infiltration in tumor tissues, particularly M2-type macrophages [9]. Additionally, the emerging role of RNA methylation in regulating immune cell infiltration into tumors has garnered attention for its potential effects on immunotherapy responses [10–12]. Despite these advances, research on the intersection of m6A, the tumor microenvironment, and glycolysis remains limited. Most prior studies have relied on cell and animal models, which might not fully capture the complexity of human tumors. A notable research gap is the lack of detailed exploration of these mechanisms in clinical patient samples, particularly in STS.

Therefore, the aim of this study was to investigate METTL3 expression through database analysis and immunohistochemistry, and to explore the possible relationships among clinicopathological characteristics, immune infiltration, and ^{18}F-FDG uptake in patients with STS.

Table 1 Summary of enrolled clinical cohort

Parameters	Classify	Cases [*n* (FNCLCC* grade I/II/III)]
Histological subtype	Liposarcoma	4 (1/0/3)
	Fibrosarcoma	6 (1/3/2)
	Synovia sarcoma	6 (0/2/4)
	Undifferentiated sarcoma	8(0/0/8)
	Leiomyosarcoma	7 (3/0/4)
	Angiosarcoma	5 (1/2/2)
	Rhabdosarcoma	1 (0/0/1)
	Extrasolar-skeletal muscle sarcoma	2 (0/2/0)
Pathology Method	Biopsy pathology	6
	Post-operative pathology	33

Notes: "*" for "French National of Cancer Research Center" grading system of soft tissue sarcoma

Materials and methods

Genomic database analysis methods

Data for samples of normal and STS tumor tissues were obtained from public genomic databases, including The Cancer Genome Atlas (TCGA) and Genotype-Tissue Expression (GTEx). A final sample of 262 STS was analyzed, with normal muscle tissue serving as a control (n=395). All data were processed to remove batch effects, thus ensuring the comparability of the two datasets. Subsequently, we analyzed METTL3 mRNA expression in STS and normal muscle tissue samples. We subsequently extracted the overall survival (OS) and survival status data from TCGA database to conduct survival analysis. The median follow-up time for the patients was 933 days. Two cases with incomplete clinical data were excluded, and a total of 260 patients were included in the analysis.

Patient selection and data management

The study adhered to the principles of the updated Declaration of Helsinki (2013 revision) and was approved by the Institutional Ethics Committee of the First Affiliated Hospital of Dalian Medical University (PJ-KS-KY-2021-249). Informed consent was waived for retrospective studies. A total of 39 patients with STS, who underwent ^{18}F-FDG PET/CT examinations at our center before treatment between January 2013 and January 2022, were retrospectively reviewed. The cohort consisted of 19 males and 20 females, with a median age of 59 years (range:32.0–84.0). Histopathological grading was based on the French Federation of Cancer Centres (FNCLCC) system [13], as summarized in Table 1.

^{18}F-FDG PET/CT imaging protocol and analysis

Approximately 60 min before imaging, they received an intravenous injection of ^{18}F-FDG at a dose of 5.55 MBq/kg. A single PET scanner (Biograph True-Point Row 64, Siemens, Germany) was used for all scans. Both CT and PET images were acquired sequentially, with a matrix size of 168×168, a tube voltage of 120 kV, automatic care-dose tube current adjustment, a range of 60–80 mAs, and a pitch of 0.8. PET imaging utilized three-dimensional acquisition mode at 1.5 min per bed position, with an axial field of view of 500 mm and a slice thickness of 5 mm. The images were reconstructed using the OSEM and PSF methods, with three iterations, 21 subsets, and

a 4 mm Gaussian filter. CT images were used for attenuation correction of the PET dataset.

The analysis was performed using a Standard MMWP workstation equipped with TureD software (Siemens Healthcare). A spherical volume of interest (VOI) was manually outlined on the tumor's largest cross-section, after which the standardized uptake value (SUV) was automatically computed. Metabolic tumor volume (MTV) was defined as the total volume of voxels within the VOI with an SUV above 2.5. Total lesion glycolysis (TLG) was calculated by multiplying MTV by the mean SUV (SUVmean). Two experienced radiologists independently conducted double-blinded evaluations and measurements.

Histopathologic staining and analysis

Two pathologists selected representative tumor tissue sections and prepared 4-μm-thick slices for immunohistochemistry (IHC) using the streptavidin-biotin method. After preparing the slides and retrieving antigens, primary antibodies were applied, followed by secondary antibodies. The slides were then stained, counterstained, dehydrated, and mounted. METTL3 was detected by membrane staining, while CD163, CD68, CD8, and CD4 were identified by staining the cytoplasm and/or membranes, with spleen tissue as a positive control [14, 15]. Images were captured at high magnification from five randomly selected regions, and protein expression was quantified using 1.48v Fiji ImageJ software [9]. The average integrated optical density (IOD) values were used for analysis.

^{18}F-FDG radioautography and image analysis

The immersion method for ^{18}F-FDG digital autoradiography, as outlined in a previous study [16], was applied. Human STS tissue sections, after being dewaxed and hydrated, were incubated in an ^{18}F-FDG PBS solution (1 MBq/mL) for 40 min at room temperature, with or without a nonradioactive reference compound (125 μg/mL). After incubation, the sections were rinsed with distilled water, air-dried, and exposed to a multisensitive phosphor screen (PerkinElmer AQ5) for 1 h. The screen was then scanned with a GE Amersham Typhoon Biomolecular Imager at 50 μm resolution. Quantitative analysis of radioactivity counts within the regions of interest (ROI) was performed using Image Quant TL 8.1 software, with maximum density (MD) as the quantitative index [17].

Statistical analysis

Statistical analyses were performed using GraphPad Prism v8.0 and R Studio. The Wilcoxon test was applied to compare METTL3 positive expression between tumor and normal tissues. Kaplan-Meier analysis was used to examine the association between METTL3 mRNA expression and overall survival in STS patients. Spearman's correlation analysis was employed to assess relationships between variables, while the Mann-Whitney U test was used to compare METTL3 expression across different clinical characteristic groups. A receiver operating characteristic (ROC) curve was generated to assess the diagnostic performance of metabolic parameters in predicting METTL3 expression. Statistical significance was defined as a p-value below 0.05.

Results

Bioinformatics analysis of METTL3 mRNA expression and the relationship between METTL3 and prognoses of patients with STS

To determine METTL3 mRNA expression in STS, we performed database analyses to compare the expression differences in METTL3 mRNA between normal tissues and STS tumor tissues. METTL3 mRNA expression was significantly upregulated in STS tissues ($n=262$) compared with normal tissues ($n=395$) ($p<0.001$). Further analysis with the Kaplan-Meier Plotter database was performed to examine the relationship between METTL3 mRNA expression and the prognosis of patients with STS. Patients with high METTL3 expression had significantly shorter overall survival than those with low METTL3 expression ($p=0.008$) (Fig. 1).

Immunohistochemical staining analysis of METTL3 protein expression in STS tumor tissues

Immunohistochemical detection was performed to assess the expression levels of METTL3 protein in STS tumor tissues versus adjacent normal tissues from clinical samples. METTL3 protein localized primarily in the nuclei of tumor cells, and displayed brown or tan staining (Fig. 2). The percentage of positive METTL3 expression in STS tumor tissues was 97.44% (38/39), a value significantly higher than the 10.0% (3/30) observed in adjacent non-tumor tissues ($p<0.001$). Across the study cohort, the median IOD value of METTL3 expression was 33974.75(9665.75-49946.92), and heterogeneity in expression levels was observed across patients.

Correlation between METTL3 protein expression and clinicopathological features in STS tumor tissues

The median ($Q1–Q3$) expression levels of METTL3 in tumor tissues of the grade III and grade I-II STS groups were 37717.11 (22300.91-51076.66) and 8833.43 (6214.66-62609.59), respectively. METTL3 expression was significantly higher in the high grade(III) group than the low grade group(I and II), and the difference was statistically significant (Z=-2.026, $p=0.043$). However, we observed no significant difference in METTL3 expression levels in tumor tissues by age, sex, tumor size, or tumor location, or between the metastatic and non-metastatic

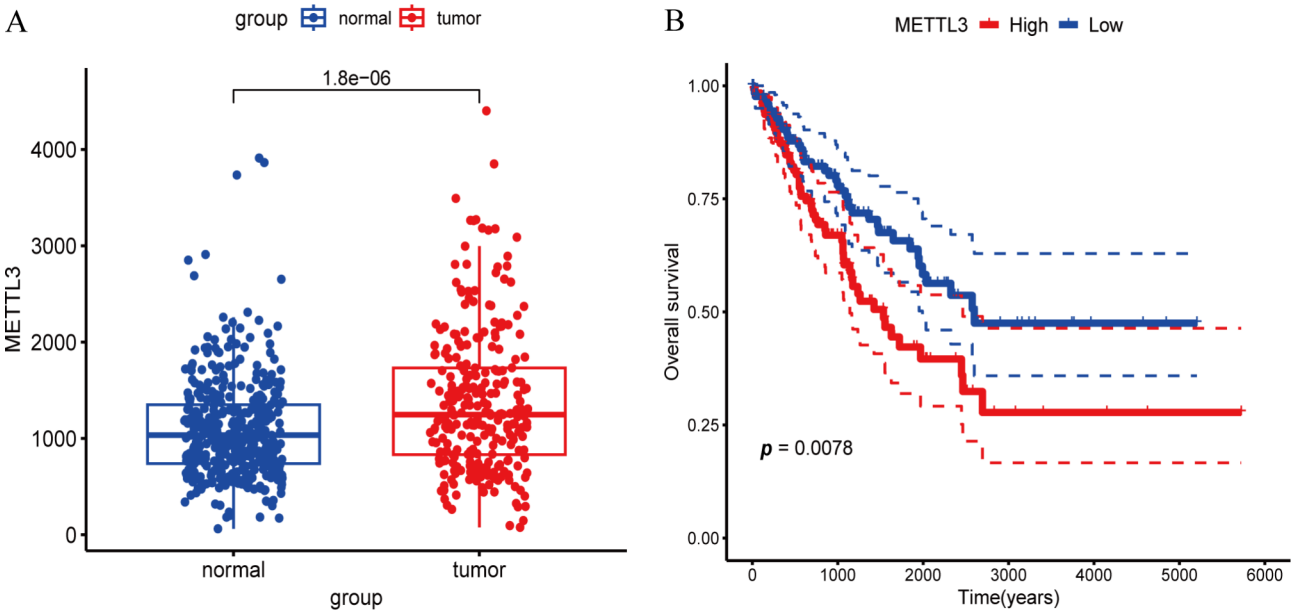

Fig. 1 Bioinformatics analysis of METTL3 mRNA expression in patients with STS. (**A**) METTL3 mRNA levels were significantly higher in STS tumor tissues than normal tissues. (**B**) Kaplan-Meier plot illustrated the correlation between METTL3 mRNA expression and survival rates in patients with STS

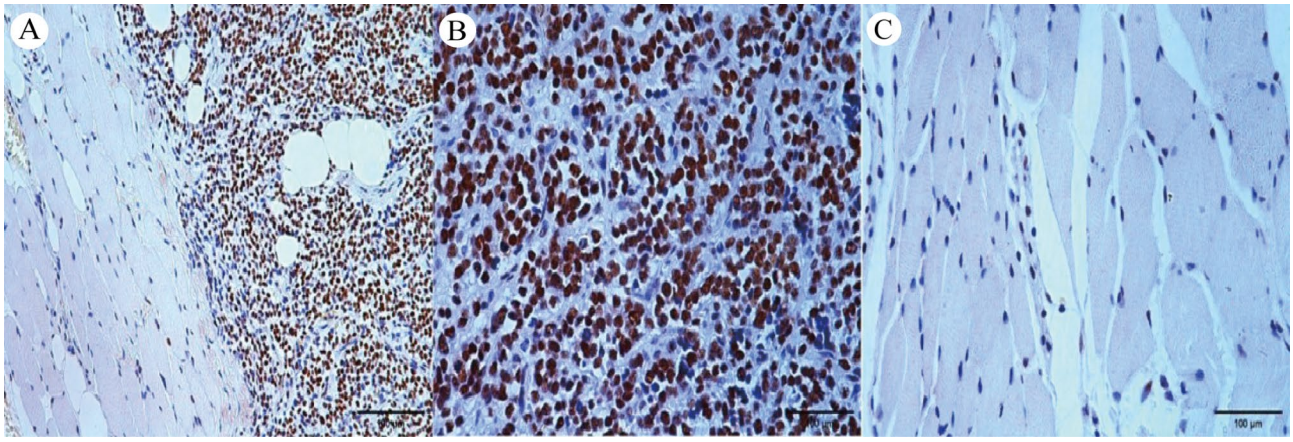

Fig. 2 Immunohistochemical staining of METTL3 in STS tissues. (**A**) Comparison of METTL3 staining differences between tumor tissues and adjacent non-tumor tissues (200× magnification). (**B**) Strong diffuse positive METTL3 staining was observed in tumor tissues, with METTL3-positive staining appearing brown and localized predominantly to the nucleus. (**C**) Negative METTL3 staining in adjacent non-tumor tissues (400× magnification)

groups (all $p$values>0.05) (Table 2). Further analysis of the correlation between METTL3 protein expression and immune cell infiltration in STS tumor tissues indicated that METTL3 expression positively correlated with the expression levels of CD163 (r=0.502, p=0.011), CD68 (r=0.381, p=0.017), and CD8 (r=0.319, p=0.048). We also observed a trend toward correlation with CD4 expression (r=0.310, p=0.055) (Fig. 3).

Correlation between METTL3 protein expression and ^{18}F-FDG metabolism in STS tumor tissues

We next measured the metabolic parameters SUVmax, MTV, and TLG on a ^{18}F-FDG PET/CT post-processing workstation for 39 patients with STS. The correlation between ^{18}F-FDG PET metabolic parameters and METTL3 protein expression in STS tissues was analyzed. SUVmax positively correlated with METTL3 expression in STS tissues (r=0.580, p<0.001). However, the correlations with MTV and TLG were not significant [r=0.198 (p=0.226) and 0.305 (p=0.059), respectively]. Further analysis was conducted on serial sections of tumor tissues from 39 STS cases, for comparative analysis of ^{18}F-FDG autoradiography and METTL3 expression. The median autoradiographic MD value obtained from STS tissue sections was 182.55 (107.73-258.35). The MD value positively correlated with the expression level of METTL3 (r=0.434, p=0.006) (Fig. 3).

Table 2 Correlation between METTL3 expression and clinicopathological features in STS

Clinicopathological Features	Cases(*n*)	METTL3 expression	
		Statistical value	*P* value
Age			
< 60 years	21	*Z*=-0.560	0.955
≥ 60 years	18		
Genders			
Male	19	*Z*=-0.365	0.715
Female	20		
Tumor size			
<5 cm	18	*Z*=-0.761	0.460
≥5 cm	21		
Tumor location			
Limbs	20	*Z* = 2.061	0.357
Trunk	10		
Thoracic and retroperitoneal	9		
FNCLCC*			
Grade I-II	14	*Z*=-2.026	0.043†
Grade III	25		
Transferred or not‡			
Concomitant metastasis	10	*Z*=-0.579	0.563
None	29		

Notes: "*" for "French National of Cancer Research Center" grading system of soft tissue sarcoma, "†" denotes statistically significant differences, "‡" indicates the presence or absence of lymph node and/or distant metastasis

The cohort was divided into a high METTL3 expression group (n=20) and a low METTL3 expression group (n=19), with the median METTL3 expression serving as the cutoff. The SUVmax of STS in the high METTL3 expression group was higher than that in the low expression group [medians of 16.16 (11.9–20.9) vs. 10.05 (5.1–14.4), Z = -2.979, p=0.003] (Fig. 4A). The area under the ROC curve for the difference in SUVmax between STS groups was 0.779 (95% CI=0.626–0.932, p=0.003) (Fig. 4B). On the basis of the maximum Youden index, the optimal threshold of SUVmax was determined to be 9.9, with a sensitivity of 81.0% and a specificity of 70.2% for predicting high METTL3 expression. Typical cases are shown in Figs. 4 and 5.

Discussion

STS, a highly invasive and difficult-to-treat disease, poses challenges such as high recurrence, metastasis rates and short survival times. In recent decades, research in malignant tumor biology has focused on tumor genetics. The m6A is the most widespread dynamic and reversible epigenetic modification of mRNA. METTL3 is a key enzyme regulating the translation efficiency and stability of specific target mRNAs [18–20]. However, whether and how METTL3 regulates the tumor microenvironment and energy metabolism in STS remains largely unknown. This study used public databases and clinical patient samples to analyze METTL3 expression in tumor tissues. The correlations of METTL3 expression in patients with STS with prognostic and clinicopathological features, as well as glucose metabolism, were further explored. METTL3 expression was significantly upregulated in STS tumor tissues, and was closely associated with high tumor histological grades and poor prognosis. Additionally, this study reports what is, to our knowledge, the first evidence of a positive correlation between high METTL3 expression in STS tumor tissues and tumor immune cell infiltration, as well as ^{18}F-FDG metabolism. Our findings highlighted the correlation between metabolic pathways with tumor biology and provided new perspectives for bridging the gap between epigenetic modifications and tumor immunity through the lens of glucose metabolism.

Aberrant epigenetic modifications can lead to gene misexpression and genetic alterations. The expression of METTL3, the core catalytic subunit involved in RNA m6A modification, was studied in STS, on the basis of TCGA, GTEx data, and IHC staining of STS clinical samples. METTL3 expression was significantly upregulated in STS tissues, and its high expression was associated with high histological grade and poor prognoses in patients with STS. This finding was consistent with those from previous studies on human malignancies such as lung adenocarcinoma and bladder cancer [21, 22], thus suggesting that METTL3 may have a potential oncogenic role in the occurrence and progression of STS.

Immunotherapy has emerged as a new approach in the treatment of malignancies but has not yet led to groundbreaking progress in STS [23]. Tumor-associated macrophages (TAMs), the most important immune cells in the tumor stroma, are considered a potential therapeutic target for tumor immunosuppressive therapy. However, the lack of understanding of the heterogeneous cell populations has limits the clinical application of TAMs [24]. Therefore, exploring relatively specific markers and functional molecules within TAMs will be crucial to further elucidate the immunosuppressive role of TAMs and develop macrophage-targeted immunotherapies.

RNA methylations, particularly m6A modifications, have been a topic of recent interest, given its potential effects on immune cell behavior and tumor progression. Differences in m6A modification patterns are an important factor contributing to the heterogeneity and complexity of individual tumor microenvironments [25, 26]. Our clinical data analysis revealed that METTL3 expression in STS tumor tissues positively correlated with immune cell infiltration markers, including CD163, CD68, CD8, and CD4, and was particularly strong with CD163. Similar studies, such as an analysis conducted by Zhen et al. using the GEPIA database, have shown that METTL3 expression in reproductive system malignancies positively correlates with CD8, CD4, and NK cell infiltration [27]. Therefore, we hypothesized that

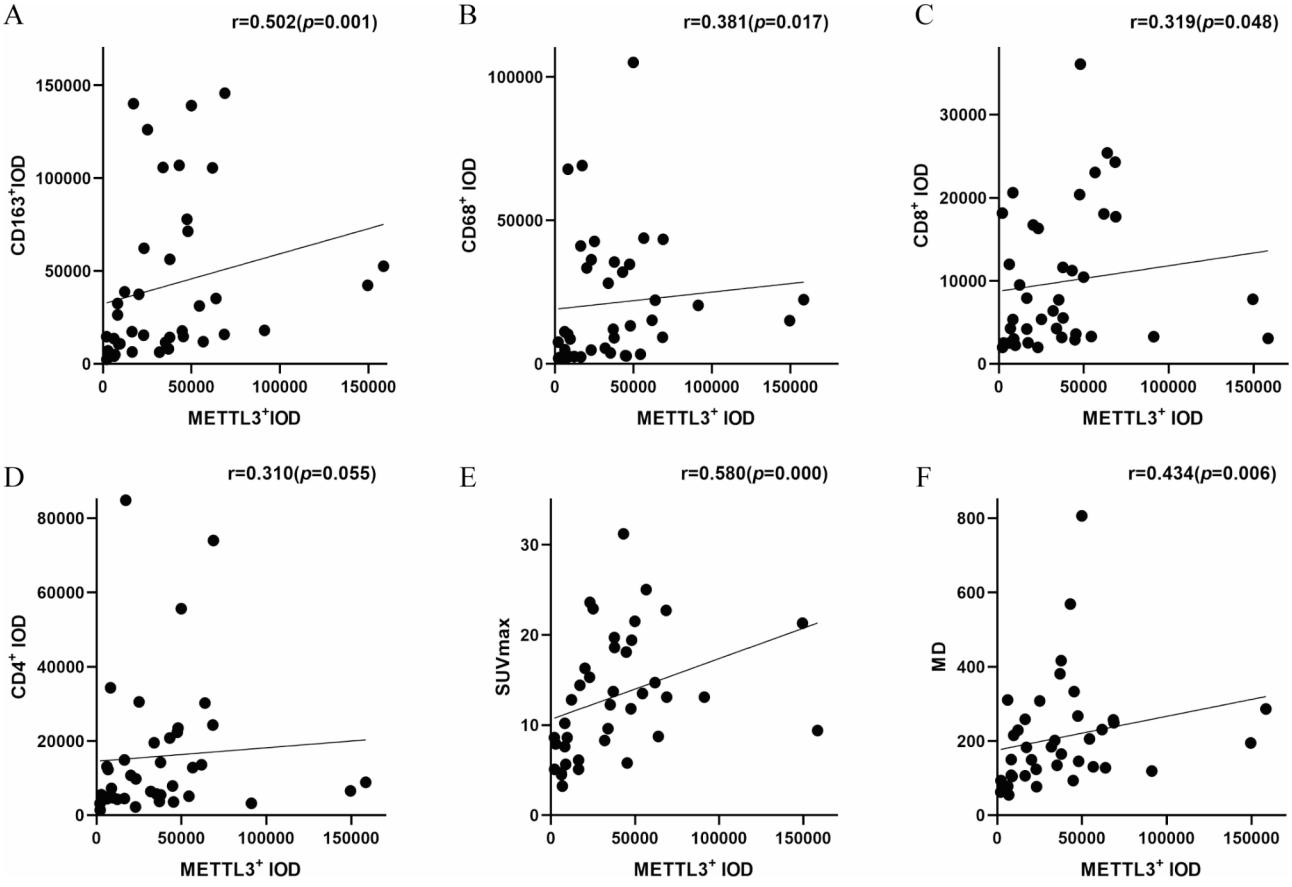

Fig. 3 Correlations among METTL3 expression, immune cell infiltration, and ^{18}F-FDG metabolic parameters. (**A-D**) METTL3 expression positively correlated with CD163, CD68, and CD8 ($r=0.532, 0.381, 0.319$; all p values <0.05 for all), and showed a positive trend toward association CD4 ($r=0.310$, $p=0.055$). (**E**) METTL3 expression positively correlated with the ^{18}F-FDG PET metabolic parameter SUVmax ($r=0.580$, $p=0.000$). (**F**) METTL3 expression positively correlated with the ^{18}F-FDG autoradiography uptake parameter MD value ($r=0.434$, $p=0.006$)

METTL3 might influence the malignant progression in patients with STS by modulating the tumor immune response. These new findings might provide new insights into how tumors adapt to their microenvironment and might be targeted more effectively with immunotherapy.

The "Warburg effect" is a hallmark of cancer metabolism and the basis of ^{18}F-FDG imaging. Our previous research has indicated that, when accounting for the characteristics of various tumor cell subtypes, the metabolic level of ^{18}F-FDG independently correlates with the expression of the M2-type TAMs marker CD163. Several studies have identified links between epigenetic factors and glucose metabolism in vitro experiments, thus suggesting that these factors influence the metabolic phenotype of tumors [28–30]. Our study revealed a significant correlation between ^{18}F-FDG metabolism in patients with STS and METTL3 expression. The SUVmax in ^{18}F-FDG PET uptake was significantly higher in the group with high rather than low METTL3 expression, in agreement with findings reported by Liu et al. [30] in esophageal squamous cell carcinoma. Additionally, we further assessed METTL3 immunohistochemistry through ex vivo autoradiography on tissue sections, which yielded similar results.

Liu et al. showed that METTL3 may affect the glycolytic pathway in tumor cells by up-regulating the expression of glucose transporter 1 and hexokinase 2, thereby increasing ^{18}F-FDG uptake [30]. Other studies found that METTL3 could increase the expression of pyruvate kinase M2 (PKM2) through m6A modification, which in turn led to the enhancement of aerobic glycolysis, tumor cell proliferation, and tumor formation in lung adenocarcinoma [31] and esophageal cancer mouse models [32]. In addition, as an important component of the tumor microenvironment, TAMs was found to have a higher glucose uptake rate compared to cancer (rectal, renal, and breast) cells themselves and other immune cells [33]. TAMs are usually abundantly clustered in hypoxic regions that are regulated by HIF-1α, and PKM2, as a coactivator of HIF-1α, plays a role in the regulation of macrophage function [34]. In conclusion, m6A modification mediated by METTL3 can promote glycolysis by inducing the expression of related enzymes and transcriptional effectors to facilitate tumor development.

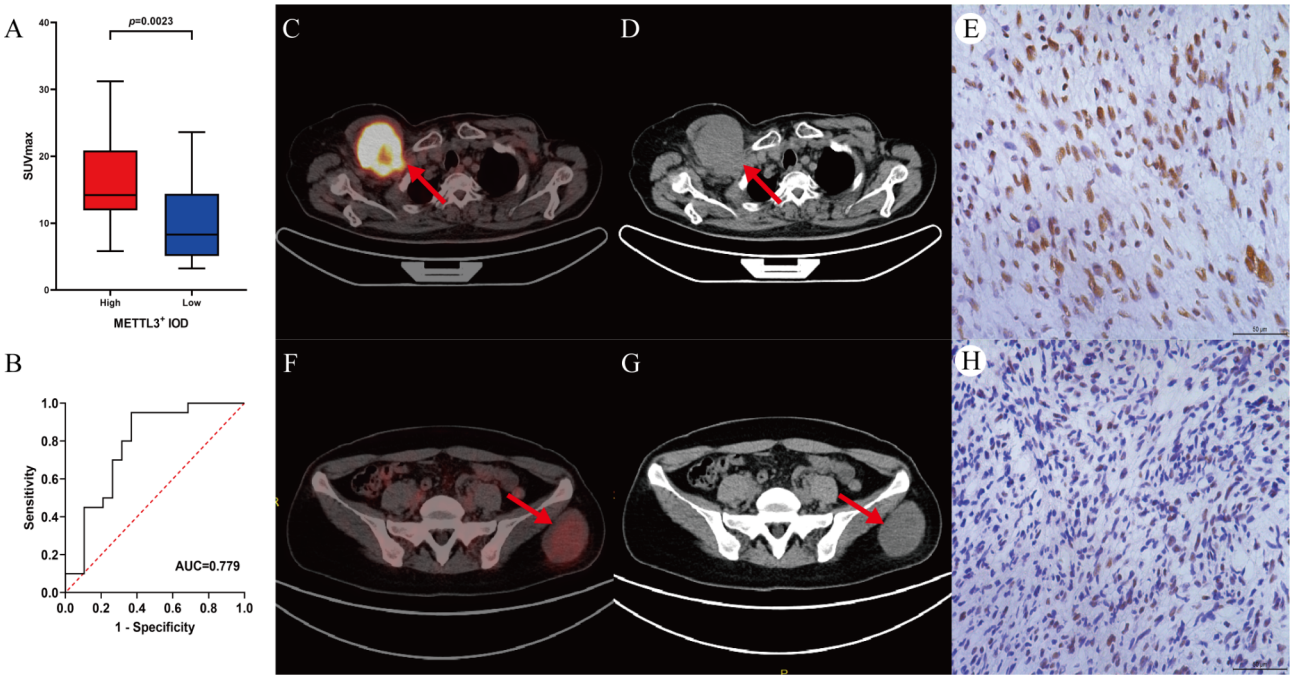

Fig. 4 Association of SUVmax with METTL3 protein expression in STS, along with case examples. (**A-B**) Box plot (Z=-2.979, p=0.003) and ROC curve [AUC=0.779 (95% CI=0.626–0.932, p=0.003)]of SUVmax comparing STS groups with low and high METTL3 expression. (**C-E**) A 73-year-old woman with undifferentiated sarcoma (FNCLCC III). As indicated by the red arrow, a soft tissue mass with a maximum diameter of 7.5 cm was visible in the right anterior upper chest wall, with markedly elevated ^{18}F-FDG uptake (SUVmax 18.1) and diffuse METTL3 positivity, IOD value was 61818.15. (**F-H**) A 39-year-old woman with leiomyosarcoma (FNCLCC I). As indicated by the red arrow, a soft tissue mass with a maximum diameter of 6.1 cm was visible within the left gluteal fat layer, with mildly elevated ^{18}F-FDG uptake (SUVmax 3.23) and scattered weak METTL3 positivity, IOD value was 6791.90

Based on the preliminary clinical observations in our study, high METTL3 expression in STS suggests poor prognosis, and the metabolic level of ^{18}F-FDG is closely related to METTL3 expression and immune infiltration, which will provide a preliminary theoretical basis for METTL3-mediated m6A modification being a meaningful therapeutic target in STS. While the potential biological mechanisms of METTL3 in STS heterogeneous immune cell infiltration and reprogramming of glucose metabolism are still unknown, we also would like to further clarify them in our future studies.

Moreover, this study reported what are, to our knowledge, the first observations of a correlation between METTL3 expression in STS tissues and the ^{18}F-FDG PET metabolic parameters MTV and TLG. Unlike SUVmax, which reflects the metabolic level of the most active part of the tumor and is usually closely related to the aggressiveness and malignancy of the tumor, MTV and TLG are usually used to assess the overall glucose metabolic load of the tumor. Although no significant correlation was found, this lack of significance might have been because epigenetic modifications in tumors occur at any stage during tumorigenesis and development [35], and there is often heterogeneity within the tumors, especially in the border regions of the tumors, which may be subjected to a more intense inflammatory response to the tumor, which may result in an overall metabolic load increases [36], but the metabolic activity in these regions may not have a direct linear relationship with METTL3 overexpression.

In summary, although the present study could not avoid the heterogeneity of STS, and potential limitations from tissue sampling errors, our findings confirmed that METTL3 expression significantly differed between STS and normal tissues. METTL3 was notably upregulated in STS tumor tissues and associated with high histological grades and poor prognosis, thus suggesting its potential involvement in STS invasiveness and progression, and its utility as a potential biomarker. Additionally, this study revealed a correlation between METTL3 expression in STS tumor tissues and high levels of immune cell infiltration, as well as a positive correlation with ^{18}F-FDG metabolism. Combined with our previous findings demonstrating positive correlations among ^{18}F-FDG metabolism, METTL3, and M2-type TAMs, we hypothesized that, during the occurrence and progression of STS, high tumor cell infiltration and elevated glucose metabolism might be associated with gene alterations induced by METTL3-mediated m6A methylation epigenetic dysregulation. Moreover, our findings provided insights that may guide the future implementation of individualized treatment regimens.

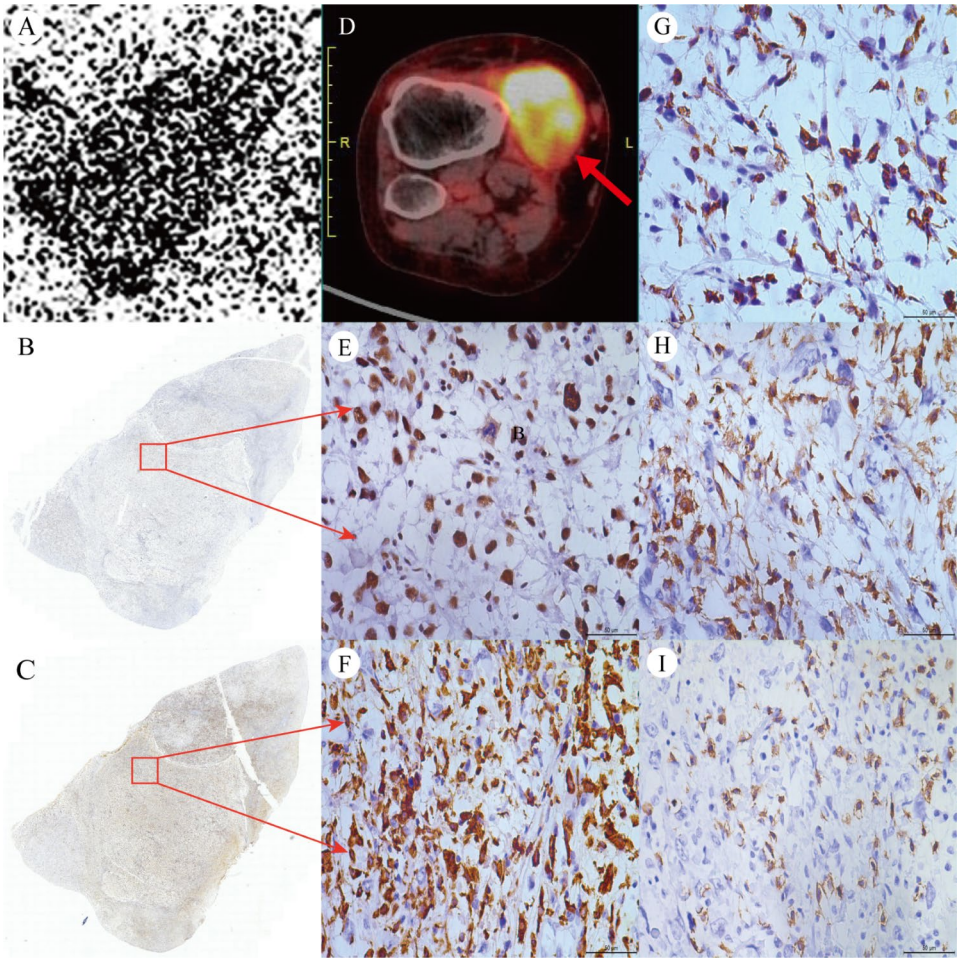

Fig. 5 Immunohistochemistry and ^{18}F-FDG PET of a patient with STS, with corresponding ex vivo ^{18}F-FDG autoradiography images. A 66-year-old woman with undifferentiated sarcoma (FNCLCC III). (**A**) ^{18}F-FDG radioautography of tumor tissue. The MD value was 248.97. (**B-C**) Scans of full section IHC pathology for METTL3 and CD163. (**D**) ^{18}F-FDG PET/CT fusion image. As indicated by the red arrow, a soft tissue density mass in the right knee joint was observed. The maximum diameter of 5.9 cm, ^{18}F-FDG uptake was markedly elevated, and the SUVmax was 13.1. (**E-I**) Magnification of pathology images of (400×) pathology images of METTL3, CD163, CD68, CD8, and CD4, with IOD values of 68863.32, 145793.57, 53432.39, 73969.214, and 17722.21. In follow-up the patient developed lung metastases at 11 months postoperatively

Conclusion

METTL3 was significantly overexpressed in STS tumor tissues and was positively correlated with high histological grades, elevated immune cell infiltration, and elevated ^{18}F-FDG metabolism. Targeting METTL3 may improve personalized treatment strategies for STS, and SUVmax may serve as a potential imaging biomarker for METTL3 expression.

Abbreviations

GTEx	Genotype-Tissue Expression
FNCLCC	French Federation of Cancer Centres
IHC	Immunohistochemistry
IOD	Integrated optical density
m6A	N6-methyladenosine
MD	Maximum density
MTV	Metabolic tumor volume
METTL3	Methyltransferase-like 3
OS	Overall survival
ROC	Receiver operating characteristic
ROI	Regions of interest
STS	Soft tissue sarcomas
SUV	Standardized uptake value
TCGA	The Cancer Genome Atlas
TLG	Total lesion glycolysis
VOI	Volume of interest
PKM2	Pyruvate kinase M2

Acknowledgements

Not applicable.

Author contributions

Conceptualization, B.C. Investigation and Methodology, T.W. and B.C. Software and Formal analysis, T.W., H.Z. and HB.F. Resources and data curation, Writing-original draft preparationn, T.W. and B.C. Writing-review and editing, visualization and supervision, JH.X, H.Z. and B.C. Project administration authors have read and agreed to the published version of the manuscript.

Funding

The study was supported by Natural Science Foundation of Liaoning Province, China (No. 2024-BS-164),and Dalian Medical Science research project, China (No.2023-DF-036).

Data availability
No datasets were generated or analysed during the current study.

Declarations

Ethics approval and consent to participate
This retrospective study was approved and the requirement for the informed consent was waived by the Institutional Review Board of the First Affiliated Hospital of Dalian Medical University, and was carried out in accordance with the Declaration of Helsinki.

Consent for publication
Not applicable.

Competing interests
The authors declare no competing interests.

Received: 23 September 2024 / Accepted: 31 December 2024
Published online: 07 January 2025

References

1. Huang ZD, Lin LL, Liu ZZ, et al. m6A modification patterns with distinct immunity, metabolism, and stemness characteristics in soft tissue sarcoma. Front Immunol. 2021;24(12):765723. https://doi.org/10.3389/fimmu
2. In GK, Hu JS, Tseng WW. Treatment of advanced, metastatic soft tissue sarcoma: latest evidence and clinical considerations. Ther Adv Med Oncol. 2017;9(8):533–5350.
3. Siegel RL, Miller KD, Fuchs HE, et al. Cancer Stat 2021 CA Cancer J Clin. 2021;71(1):7–33. https://doi.org/10.1177/1758834017712963
4. He L, Li H, Wu A, et al. Functions of N6-methyladenosine and its role in cancer. Mol Cancer. 2019;18(1):176. https://doi.org/10.1186/s12943-019-1109-9
5. Wright CM, Halkett G, Carey Smith R, et al. Sarcoma epidemiology and cancer-related hospitalisation in Western Australia from 1982 to 2016: a descriptive study using linked administrative data. BMC Cancer. 2020;20(1):625. https://doi.org/10.1186/s12885-020-07103-w
6. Ansari I, Chaturvedi A, Chitkara D et al. CRISPR/Cas mediated epigenome editing for cancer therapy. 2022;83:570–83. https://doi.org/10.1016/j.semcancer
7. Xu Y, Song M, Hong Z, et al. The N6-methyladenosine METTL3 regulates tumorigenesis and glycolysis by mediating m6A methylation of the tumor suppressor LATS1 in breast cancer. J Exp Clin Cancer Res. 2023;42(1):10. https://doi.org/10.1186/s13046-022-02581-1
8. Cai J, Cui Z, Zhou J, et al. METTL3 promotes glycolysis and cholangiocarcinoma progression by mediating the m6A modification of AKR1B10. Cancer Cell Int. 2022;22(1):385. https://doi.org/10.1186/s12935-022-02809-2
9. Chen B, Tao J, Wu T, et al. Correlation between ^{18}F-FDG PET-derived parameters and quantitative pathological characteristics of soft tissue sarcoma. Quant Imaging Med Surg. 2023;13(12):7842–53. https://doi.org/10.21037/qims-23-412
10. Guo Y, Heng Y, Chen H, et al. Prognostic values of METTL3 and its roles in Tumor Immune Microenvironment in Pan-cancer. J Clin Med. 2022;12(1):155. https://doi.org/10.3390/jcm12010155
11. Deng X, Sun X, Hu Z, et al. Exploring the role of m6A methylation regulators in glioblastoma multiforme and their impact on the tumor immune microenvironment. FASEB J. 2023;37(9):e23155. https://doi.org/10.1096/fj.202301343
12. Xiao KW, Yang ZQ, Yan X, et al. Molecular characteristics of m6A regulators and Tumor Microenvironment Infiltration in Soft tissue sarcoma: a gene-based study. Front Bioeng Biotechnol. 2022;19(10):846812. https://doi.org/10.3389/fbioe
13. Sbaraglia M, Dei Tos AP. The pathology of soft tissue sarcomas. Radiol Med. 2019;124(4):266–81. https://doi.org/10.1007/s11547-018-0882-7
14. Liu XS, Zhang Y, Liu ZY, et al. METTL3 as a novel diagnosis and treatment biomarker and its association with glycolysis, cuproptosis and ceRNA in oesophageal carcinoma. J Cell Mol Med. 2024;28(6):e18195. https://doi.org/10.1111/jcmm.18195
15. Tamma R, Ingravallo G, Annese T, et al. Tumor Microenvironment and Microvascular Density in Follicular Lymphoma. J Clin Med. 2022;11(5):1257. https://doi.org/10.3390/jcm11051257
16. Li C, Zhang P, Nie R, et al. Targeting amyloids with [18F]AV-45 for medullary thyroid Carcinoma Positron Emission Tomography/Computed Tomography Imaging: a Pilot Clinical Study. Mol Pharm. 2022;19(2):584–591. https://doi.org/10.1021/acs.molpharmaceut.1c00680
17. Topart C, Werner E, Arimondo PB. Wandering along the epigenetic timeline. Clin Epigenetics. 2020;12(1):97. https://doi.org/10.1186/s13148-020-00893-7
18. Zhao R, Chen J, Wang Y, et al. Prognostic roles of dysregulated METTL3 protein expression in cancers and potential anticancer value by inhibiting METTL3 function. Fundamental & clinical pharmacology. Fundam Clin Pharmacol. 2024;7. https://doi.org/10.1111/fcp.13020
19. Chaojun Y, Xiong J, Zhou Z, et al. A cleaved METTL3 potentiates the METTL3-WTAP interaction and breast cancer progression. ELife. 2023;12. https://doi.org/10.7554/eLife.87283
20. Ivan Corbeski et al. Pablo Andrés Vargas-Rosales, Rajiv Kumar Bedi,. The catalytic mechanism of the RNA methyltransferase METTL3[J]. ELife. 2024; 12. https://doi.org/10.7554/eLife.92537
21. Yang Z, Shen Z, Jin D, et al. Mutations of METTL3 predict response to neoadjuvant chemotherapy in muscle-invasive bladder cancer. J Clin Translational Res. 2021;7(3):386–413.
22. Zhang Y, Liu X, Liu L, et al. Expression and prognostic significance of m6A-Related genes in Lung Adenocarcinoma. Med Sci Monit. 2020;26:e919644. https://doi.org/10.12659/MSM.919644
23. Petitprez F, de Reyniès A, Keung EZ, et al. B cells are associated with survival and immunotherapy response in sarcoma. Nature. 2020;577(7791):556–60. https://doi.org/10.1038/s41586-019-1906-8
24. Fujiwara T, Healey J, Ogura K, et al. Role of Tumor-Associated macrophages in Sarcomas. Cancers (Basel). 2021;13(5):1086. https://doi.org/10.3390/cancers13051086
25. Luo Y, Sun Y, Li L, Mao Y. METTL3 may regulate testicular germ cell tumors through EMT and Immune pathways. Cell Transpl. 2020;29:963689720946653. https://doi.org/10.1177/0963689720946653
26. Zhang B, Wu Q, Li B, et al. M (6)a regulator-mediated methylation modification patterns and tumor microenvironment infiltration characterization in gastric cancer. Mol Cancer. 2020;19(1):53. https://doi.org/10.1186/s12943-020-01170-0
27. Zhen J, Ke Y, Pan J, et al. ZNF320 is a hypomethylated prognostic biomarker involved in immune infiltration of hepatocellular carcinoma and associated with cell cycle. Aging. 2022;14(20):8411–36. https://doi.org/10.18632/aging
28. Xue L, Li J, Lin Y, et al. m6A transferase METTL3-induced lncRNA ABHD11-AS1 promotes the Warburg effect of non-small-cell lung cancer. J Cell Physiol. 2021;236(4):2649–58. https://doi.org/10.1002/jcp.30023
29. Su H, Wang S, Soares F et al. RNA N6-Methyladenosine Methyltransferase METTL3 Facilitates Colorectal Cancer by Activating the m6A-GLUT1-mTORC1 Axis and Is a Therapeutic Target. Gastroenterology, 2021;160(4):1284–1300.649–2658. https://doi.org/10.1053/j.gastro
30. Liu XS, Yuan LL, Gao Y, et al. Overexpression of METTL3 associated with the metabolic status on 18F-FDG PET/CT in patients with esophageal carcinoma. J Cancer. 2020;11(16):4851–4860. https://doi.org/10.7150/jca.44754
31. Wang A, Zeng Y, Zhang W, et al. N6-methyladenosine-modified SRPK1 promotes aerobic glycolysis of lung adenocarcinoma via PKM splicing. Cell Mol Biol Lett. 2024;29(1):106. https://doi.org/10.1186/s11658-024-00622-5
32. Wang W, Shao F, Yang X, et al. METTL3 promotes tumour development by decreasing APC expression mediated by APC mRNA N6-methyladenosine-dependent YTHDF binding. Nat Commun. 2021;12(1):3803. https://doi.org/10.1038/s41467-021-23501-5
33. Reinfeld BI, Madden MZ, Wolf MM, et al. Cell-programmed nutrient partitioning in the tumour microenvironment. Nature. 2021;593(7858):282–288.
34. Hou PP, Luo LJ, Chen HZ et al. Ectosomal PKM2 Promotes HCC by Inducing Macrophage Differentiation and Remodeling the Tumor Microenvironment. Mol Cell. 2020;78(6):1192–1206.e10. https://doi.org/10.1016/j.molcel.2020.05.004
35. Dumars C, Ngyuen JM, Gaultier A, et al. Dysregulation of macrophage polarization is associated with the metastatic process in osteosarcoma. Oncotarget. 2016;7(48):78343–78354. https://doi.org/10.18632/oncotarget
36. Jia Q, Wang A, Yuan Y et al. Apr. Heterogeneity of the tumor immune microenvironment and its clinical relevance. Experimental hematology & oncology vol. 11,1 24. 23 2022, https://doi.org/10.1186/s40164-022-00277-y

Publisher's note